Fuel Gas Explosion Guidelines - the Congestion Assessment Method

J.S. Puttock

Shell Research Limited, Thornton Research Centre, P.O. Box 1, Chester CH1 3SH

In 1991, Cates(1) presented guidelines for the prediction of the overpressure which could be produced by a vapour cloud explosion in congested plant. These were included in the new I.Chem.E. Overpressure Monograph (2). The method gives a clear procedure for estimating the overpressure generated at the source, and includes a realistic rate of pressure decay away from that source. This has now been extended by computation, by analysis of the extensive data from the CEC-sponsored MERGE project, and by consideration of a wider range of fuels. Calculations are used to give better guidance for the pressure decay, particularly when the source pressure is above 1 bar. The data analysis also allows simple expressions to be given for the shape of the (positive) pressure wave, and for the duration of the pulse.

INTRODUCTION

For any plant containing flammable materials which might be released to form a vapour cloud, it is important to be able to estimate the consequences of the ignition of such a release. Various methods exist for the prediction of the overpressure that could be generated by a vapour cloud explosion in congested plant. These include complex computational methods, which are the subject of much research at present. However, the use of such methods is very time-consuming, and there is a great need for simpler approaches which can be used on a routine basis. A number of such methods exist and are discussed here, together with some extension and revision of the approach of Cates (1). This method provides an estimate of source pressure from a consideration of the congestion provided by plant and equipment and thus has been named the "Congestion Assessment Method".

The method was developed not as a summary of findings in a field where all the answers are known. It rather is an attempt to provide some guidance on the basis of current knowledge in a field which is still the subject of active research. In industry, decisions have to be made routinely about potential hazards. It is clearly better that guidance is available so that rational decisions can be made and so that money which is spent with the intention of improving safety is applied in the most effective way.

Another paper in this conference (3) demonstrates the success of the method in analysis of a number of large vapour-cloud explosions incidents which have occurred in recent years. It also illustrates another area where such guidance is needed - in the estimation of maximum possible loss for insurance purposes.

A number of major incidents have demonstrated that chemical plant can pose significant explosion hazards. While aiming on the side of conservatism the method attempts to identify types of plant which present less severe hazards. Knowing what constitutes less hazardous plant means that such plant has the benefit of reduced need to mitigate against hazards and reduced insurance costs. Such rewards for safer plant should in themselves produce a trend to less hazardous plant being built in the future.

BACKGROUND

This paper is concerned with vapour-cloud explosions in congested regions. In discussing explosion potential, it is useful to make a distinction between "confinement" and "congestion". An explosion in a building is confined by the walls of the building, which restrict the escape of the extra volume of gas generated by combustion. Such burning in a completely enclosed building will produce an overpressure of about 8 bars because of this volume generation. Even if there are vents in the walls (partial confinement), high pressures may still be generated because the gas cannot flow fast enough through the vents to relieve

the pressure. Explosions in areas which are more than 60% enclosed by a combination of walls or other obstructions are beyond the scope of this paper. Other methods exist for these cases, such as the Shell's SCOPE model*.

Even where there is little confinement, high pressures may be generated by congestion. Consider a vapour cloud ignited in an area containing obstacles such as pipework or process vessels. As the gas pushed forward by the expanding flame encounters the obstacles, the flow is likely to become turbulent. When the flame reaches the turbulent region, it burns faster, generating a faster flow; this faster flow produces stronger turbulence as it reaches more obstacles, in turn increasing the burning rate, and so on. The high velocities associated with the rapid burning are sufficient to generate high pressure, i.e. an explosion.

Understanding of the mechanism described above allows us to characterise the types of plant likely to cause high overpressures. These are typically chemical or refinery plant with large amounts of pipework or other obstructions. Locations where obstacles block more than 40% of the path a flame may have to travel through, or where there are closely repeated rows of obstacles are particularly bad. On the other hand, lightly congested plant no longer needs to be treated as if were as hazardous as the most congested regions. Furthermore, since the explosion is generated only by the confined region, the volume of the explosion source is related only to the volume of the congested region, not the whole flammable cloud. This means that the overpressures experienced at a distance are lower than they would be if derived from a larger dispersing cloud.

Methods

The various methods which have been used for the prediction of overpressures associated with such explosions have been discussed by Cates (1). The main points will only be reiterated briefly here.

The first method which was tried, and used for many years, was the analogy with TNT explosions. However, it is important to emphasise that the TNT equivalence method is not appropriate for vapour-cloud explosions. The pressure decay from a TNT detonation is faster than the acoustic wave from a vapour-cloud deflagration; so, if the method is arranged to give the correct pressure at one distance, the predictions at all other distances will be wrong.

A considerable advance was made with TNO's multi-energy method [5,6]. This recognised that it is the volume of the congested region which is important in determining the extent of the explosion source. Pressure decay curves are given in the method which were computed for an initially acoustic pressure wave driven by an idealised piston. It will become clear where this paper suggests a different treatment of various aspects of the modelling, but the general approach followed here is similar to that of the multi-energy method.

The main difficulty with using the multi-energy method is that it does not provide any means of estimating the pressure generated by the explosion at its source. In the absence of information, there is tendency to use a conservative estimate; so the usual recommendation is to use the curve numbered 7 in TNO's pressure decay graphs, which is equivalent to assuming a source pressure of one bar.

The "fuel gas explosion guidelines" of Cates (1) comprised the first method to provide some guidance for the estimation of the source pressure. These guidelines include a decision tree which allows estimation of the source pressure from the nature of the obstacles and the flammable gas involved. It was recognised that there are considerable uncertainties in the estimation; nevertheless sufficient is known to indicate what levels of congestion are open enough for the explosion overpressure to be significantly below one bar. Such a simple method cannot provide accurate predictions, but is intended to be conservative.

---

* *SCOPE is a physically-based computer model for vented, confined and congested explosions; it has been developed from the method described in Reference 4.*

This paper represents an update of the method presented by Cates, on the basis of more recent experiments and calculations.

OVERVIEW

The method has three stages:

1) First, the geometry of the congested region is studied to assign a reference pressure P_{ref}, which is the estimated maximum pressure which could be generated by ignition of a propane release in that geometry;

2) The influence of the reactivity of the fuel is evaluated by determining a "fuel factor" F for the fuel. P_{ref} is multiplied by F to determine the maximum source pressure P_0 for that geometry and fuel. Cates suggested a fuel factor for one common reactive gas: 2.5 for ethylene; this is extended here to a more comprehensive list.

3) The final stage is to calculate the pressure which would be experienced at a receptor some distance away from the explosion source. Cates used a simple decay law inversely proportional to distance. While this is reasonable for source pressures up to about 1 bar, it can be unduly conservative for the highest source pressures which might occur. An alternative is suggested here.

In addition, in order to assess the effect of the explosion pressure on a structure, it is often desirable to know about the duration of the pressure pulse and its shape. Correlations for these parameters are presented later in this paper.

The MERGE experiments

Several of the new aspects presented in this paper are derived from analysis of the data from the MERGE experiments. MERGE (Modelling and Experimental Research into Gas Explosions) was a collaborative project, part funded by the Commission of the European Communities (7), involving eight organisations from five European countries. Among the experiments carried out in this project was a series of explosions in unconfined but highly congested regions consisting of orthogonal arrays of intersecting pipes. Four different configurations of pipes were used, at three different scales. The congested regions extended over the volume of a half-cube, located on the ground, of dimension 2m (small scale), 4.5 m (medium scale) or 9m (large scale). The small-scale experiments were performed by TNO in the Netherlands, and the medium and large by British Gas (8,9).

The half-cubes were filled with a uniform stoichiometric mixture of gas and air (sometimes with oxygen enrichment) and ignited centrally at the ground. Gases used were methane, propane, ethylene, a methane/ propane mix and (once) acetylene.

THE COMPONENTS OF THE METHOD IN DETAIL

Reference pressure

The determination of the reference pressure, P_{ref}, is still the most difficult and uncertain part of the method. The decision tree devised by Cates was based on data in references (10) and (11) and other experiments performed by Shell Research. This is reproduced in the Appendix. In essence, it has not been changed. When further experimental data on congested vapour cloud explosions are available, it should be possible to suggest refinements to the decision tree. It is, however, encouraging to observe that the detailed assessment of a number of major incidents, presented by Barton (3), provides some confirmation of the predictions.

It is worth noting, incidentally, that the upper limit of one bar imposed on P_{ref} is not a value which it is theoretically impossible to exceed. Very high congestion, as was used in some of the MERGE experiments, can produce pressures of several bars with propane or even incipient detonation with ethylene. (Note that, in some of the MERGE experiments, there were fifteen rows of obstacles to be passed from the centre to the edge of the array.) Thus the method is based on some knowledge of the maximum levels of plant congestion typically found in refineries and chemical processing plant. The upper limit in the method is a level which is unlikely to be exceeded for the more congested examples of such plant; that is, no more than about six successive rows of obstacles, and the spacing parameter S no lower than about 7.

Fuel factor

As mentioned above, Cates indicated the need to take a source pressure different from P_{ref} for one common gas which is significantly more reactive than propane, i.e. ethylene. There are, of course, various gases which are more reactive, as well as some fuels which are less reactive.

The key to determining the fuel factor F lies in the fractal scaling theory of Taylor and Hirst (12). This predicts that the turbulent burning velocity, in a given configuration, will be proportional to the product of the laminar burning velocity and the expansion ratio of the gas raised to the power 1.36. In a fixed geometrical configuration, the overpressure will be proportional to the turbulent burning velocity squared, and thus proportional to the above product to the power 2.72.

In the MERGE project, all of the experimental configurations were tested with more than one gas; so there are many cases, over the three scales, which quantify the pressure ratios relating to changing fuel in the same configuration. The full set of data has been compared with the predictions of the fractal scaling theory by Mercx et al. (9). The agreement was excellent. This theory is therefore ideal for deriving the fuel factor F.

Such calculations have been performed for a variety of gases. Laminar burning velocities were obtained from a variety of sources; expansion ratios were derived from computed adiabatic flame temperature. The gases were found to fall roughly into a number of groups of similar fuel factor (i.e. ratio of overpressure to that derived for propane). The rounded values for each group are given in Table 1.

As an example, based on the best available data on laminar flamespeeds, the ratio of overpressure in an ethylene explosion to that for propane in the same geometry is calculated to be 2.79. In the MERGE experiments, the average ratio (over 5 pairs of experiments) was 2.83. This is rounded to 3 in Table 1.

Pressure decay

The external decay of pressure can be studied by an analysis of the external pressure measurements in the MERGE medium- and large-scale experiments. The sensors were located at 12m and 24m from the centre of the congested region, with an additional location at 4m in some experiments.* The maximum pressures obtained at 12m are plotted against the source pressure in Figure 1a. (The source pressure is the maximum over time measured in the congested region; this was very uniform across the congested region.) Equivalent results for the 24m location are shown in Figure 1b.

If the data from 12m and 24m for lower source pressures are examined in detail (Figure 2a), as well as all the measurements at 4m (Figure 2b), it can be seen that all the pressures are fitted well by the relation $P = (R_0/r)\,P_0$ (see Appendix), using a source radius $R_0 = 3.05$m. This relation is also shown as the steep lines in Figure 1. However, beyond a certain point the pressures are lower than would be derived from the

* *For convenience, all dimensions mentioned in this section refer to the medium-scale experiments; values should be doubled for the large scale.*

$1/r$ pressure decay; this is a result of faster decay due to dissipation in a shock front at the leading edge of the wave. If the multi-energy hypotheses were correct then beyond the transition point the pressure at a given distance would be independent of source pressure. (The multi-energy curves coincide after the transition point.) In fact, there is still a significant rate of increase of the pressure at 12m (and 24m) as the source pressure increases. The gradient of the best-fit line to the, rather scattered, data beyond transition is the same for both figures; these lines are plotted.

Measurements at two distances are not enough to define a complete curve for pressure decay with distance, so another approach is needed to fill the gap. This is provided by numerical modelling of the pressure decay. The calculations were performed by Hulek and Lindstedt (13) using a second-order finite-volume method with local grid refinement. Since the computations could be performed in one dimension, using spherical symmetry, a high degree of accuracy was possible. The pressure wave in the calculations was driven by a "spherical piston" with a velocity-time history chosen so that the pressure pulse as measured just outside the source region was fitted.

This approach is very similar to that used by TNO in the derivation of the pressure decay curves in the multi-energy method. The main difference is that, in the absence of realistic source pressure-time data, TNO's method assumed a constant velocity piston. The pressure wave from a constant-velocity piston develops a shock sooner, and so starts the more rapid pressure decay sooner than for a real source.

The first two pressure decay calculations used the near-source data from MERGE large-scale experiments L5 and L6, corresponding to source pressures of 1.0 bar and 2.4 bar. The predictions could therefore be validated against the measurements at the further sensors. One of these is shown in Figure 3. It can be seen that the numerical model provides a very good representation of the development of the pressure wave. Three further computations were performed with the input pressure of L5 multiplied by 3, 5 and 8, corresponding roughly to source pressures of 3, 5 and 8 bar. The exact source pressure for these cases is not known, since at the higher pressures, there would have been a faster decay from the source to the reference location for the calculations. The resolution of this ambiguity is discussed below.

When the calculated peak pressure was plotted against distance, it was noted that, apart from the slower decay near the source, the curves for all four source pressures could be made to coincide just by shifting laterally. (See Figure 4). This suggests that the rapid part of the pressure decay can be represented by the universal curve in Figure 4 with an appropriate lateral shift. The earlier part of the decay is a simple acoustic wave and so can still be represented by the $1/r$ line.

The problem still remains to determine the appropriate lateral shift for each source pressure. Fortunately, this can be derived from the MERGE data. The gradient of the shallower lines in Figures 1 and 2 provides the information needed to place the curves.

For convenience, the common pressure decay curve in Figure 4 has been represented by fitting a polynomial (on the logarithmic plot); this is an accurate representation of the computed curves from the highest pressures down to 10 mbar. Thus the final specification of the full pressure decay curves is as follows.

Let the source pressure be P_0 bar, and the effective source volume V. (The derivation of V is discussed in the Appendix.) Consider a receptor at a distance r' from the *edge* of the congested region. Then define:

$$R_0 = \sqrt[3]{\frac{3V}{2\pi}} \qquad \text{... (1)}$$

$$r = R_0 + r' \qquad \text{... (2)}$$

$$\log P_1 = 0.08l^4 - 0.592l^3 + 1.63l^2 - 3.28l + 1.39 \qquad \text{... (3)}$$

where $l = \log \frac{r}{R_0} + 0.2 - 0.02 \times P_0$ (N.B. logarithms to base 10)

Then the pressure in bars at the receptor is

$$P = \min\left(\frac{R_0}{r}P_0, P_1\right) \quad \ldots (4)$$

The curves are plotted for a number of source pressures in Figure 5. They are similar in shape to the multi-energy curves, but the point at which the faster decay commences is different, and the curves do not all coincide after transition.

The curve derived from the simple representation in Equations 3 and 4 is compared with the full computed decay curve for the 2.4 bar source pressure in Figure 6.

In the curves of Figure 5, although the shape is similar to the multi-energy curves, the faster decay starts later. This is a result of the more realistic behaviour of the "spherical piston" representing the source, which we have now been able to base on the experimental data. It can be seen in Figure 5 that at 1 bar source pressure the $1/r$ pressure decay extends to about nine times the source radius. For lower source pressures, the $1/r$ extends much further. Thus, for pressures up to 1 bar, the simple $1/r$ assumption of Cates was reasonable, although in the far field the pressures calculated now would be lower. For a source overpressure greater than 1 bar there can be a significant difference. For example, where P_0 =2.5 bar, the predicted overpressure at seven times the source radius is half that given by the $1/r$ relation.

Pulse duration and shape

If estimated pressures are to be used with structural response calculations, then information is needed on the duration of the pressure pulse and its rise time. The TNO multi-energy papers [5, 6] provide a series of curves for the duration. However, the data from the MERGE experiments can be reduced to very simple but adequate expressions for both the duration and rise time.

For each pressure sensor trace outside the congested region in the MERGE medium- and large-scale data, a triangle was fitted. An example is shown in Figure 7. The triangle is a best representation of the positive part of the pressure pulse, fitted by eye. The later negative part of the pulse is more difficult to analyse, being influenced by any baseline drift in the sensors. Defining the times t_1, t_2 and t_3, as shown in Figure 7, the pulse is defined by the peak pressure, already determined above, and a duration and "shape factor". $(t_3 - t_1)$ is the duration and $(t_2 - t_1) / (t_3 - t_1)$ is denoted the shape factor, which is the ratio of the rise time to the duration; this becomes zero as the front of the wave becomes fully shocked.

It might be expected that the duration should be related to the radius of the source, which is R_0, divided by some flame velocity scale in the explosion. This latter can be expected to be proportional to $P_0^{1/2}$. i.e. we should consider a time scale

$$\frac{R_0}{\sqrt{P_0/\rho_a}}$$

The rate of change of the pressure wave shape is much greater for higher pressures. The derived values of the duration and shape factor were found to collapse very well when plotted against the distance scaled by the square of the source pressure in each explosion; i.e. using a distance parameter:

$$d_f = \frac{r'}{R_0}\left(\frac{P_0}{P_a}\right)^2 \quad \ldots (5)$$

where r' is the receptor distance from the centre of the explosion
P_a is atmospheric pressure.

Then the duration can be related to the above time scale by a coefficient C, which has the value 0.65 in the near field, but rises after d_f = 5 to reach a value of 1.3 (Figure 8), i.e.

$$t_3 - t_1 = C\frac{R_0}{\sqrt{P'_0/\rho_a}} \qquad \ldots (6)$$

$$C = \begin{cases} 0.65 & d_f < 5 \\ 0.65\left(\frac{d_f + 10}{15}\right) & 5 < d_f < 20 \\ 1.3 & 20 < d_f \end{cases} \qquad \ldots (7)$$

Note that the maximum pressure has been denoted P'_0 here to emphasise the fact that *consistent units must be used*, e.g. when using SI units P'_0 must be in Pascals, i.e. bars multiplied by 10^5. Equation 6 is not valid inside the explosion source.

The shape factor is well represented by taking a linear decay with distance (see Figure 9):

$$\frac{t_2 - t_1}{t_3 - t_1} = max(0.65\,(1 - 1.25d_f), 0). \qquad \ldots (8)$$

From the simple expressions in Equations 6 and 8, a good, if slightly idealised, representation of the positive pressure pulse can be obtained.

It should be noted that the positive overpressure pulse is followed by a negative pulse (rarefaction) typically of lower amplitude and longer duration. This may in some circumstances be as damaging as the positive pulse.

SPECIAL CONSIDERATIONS

Other gases and gas mixtures

It should be noted that there are gases which are more reactive than those listed in Table 1, for example acetylene (ethyne) and hydrogen. These, if released in pure form, would present a greater hazard than those in the Table. However, hydrogen, in particular, is more often used mixed with other gases.

The behaviour of gas mixtures is still the subject of study. Nevertheless, it is not true, as has been suggested, that two or three per cent of a more reactive gas in a mixture is enough to increase the explosion severity to that associated with the pure reactive component. Preliminary data from some experiments which we have performed show that about 10% (molar) hydrogen in methane is needed to make the mixture as vigorous as pure propane, and 40% hydrogen is needed before the mixture behaves like ethylene. For methane/propane mixes, the pressure increase is initially faster than linear in the propane content, but it still needs 10% propane in the mix to obtain a pressure which is halfway between the methane and propane levels (i.e. $F = 0.8$).

"Bang-box" ignition

The pressure estimates derived using the guidelines in the Appendix would not apply in the case of high-energy ignition, which could increase the overpressure considerably. One such source of high-energy ignition which could be easily overlooked is a "bang-box". We use this term to refer to the ignition of gas inside a small, nearly-enclosed area. If such a nearly-enclosed volume vents into or near a congested region, the overpressures resulting could be very high, and detonation cannot be ruled out.

Hazard areas should be searched for potential "bang boxes". If such is identified and it vents into a fairly uncongested area, $P_{ref} = 1$ should be used in the calculation in the Appendix; if it vents towards a congested area, the result should be taken as $P_0 = 8$. The volume V used in the calculation should include everywhere within ten metres of a potential bang-box.

THE METHOD IN PRACTICE

We can now discuss how the Congestion Assessment Method is used in making an estimate of possible explosion overpressure in a particular area in, say, a refinery or chemical processing plant. In making such an assessment, there is no substitute for walking round the plant. Once there, the normal strategy is to walk into the darkest region in the middle of the plant. The area where little daylight reaches is normally the place from which a flame would have to pass the most congestion. From the position where equal congestion must be passed to the outside in both directions, count the number of obstacle layers to the outside. Defining what constitutes an obstacle layer is difficult, and no easy help can be given in this. The ambiguity in this area illustrates the uncertainty of the method - the result will be rough guidance on the likely maximum overpressure, not a precise calculation.

In determining the congestion parameter S_1 (see Appendix), it is often easier to use the blockage ratio, b, where b is the proportion of the cross-section blocked by the obstacle layer. All obstacles which are being taken as one layer should be added in. A certain amount of calculation is desirable, since most people's rough estimates of blockage ratio are too low. Then the parameter S_1 can be calculated from

$$S_1 = \frac{1}{b} - 1$$

S_2 is usually best calculated directly from the spacing between the obstacle layers, and the typical obstacle diameter.

At some stage it is important to check whether some part of the area is excessively confined. Where there is a solid slab above process units, it is easily possible for the fully blocked roof plus the partial blockage by the densest obstacle layer at each side to exceed 60% of the sum of the area of the roof plus the four sides.

If the volume passes that test, then it is relatively straightforward to use the decision tree in the Appendix to obtain P_{ref} and apply the fuel factor, leading to P_0, and from that to derive the pressure P at any distant location.

It must be remembered that P is the static pressure in the expanding pressure wave. In considering the interaction with a building, for example, a wall of the building facing the explosion will experience a peak pressure about twice this value owing to reflection of the pressure wave (or somewhat more than twice if the wave is shocked, i.e. when the shape factor is zero). In addition, for a distance less than one source radius (R_0) from the edge of the hazard zone, allowance should be made for the extension of the source explosion beyond the congested region to occupy the volume V. In this region there may will also be a significant effect of dynamic pressure on the face of a building; this results from the outward flow generated by the explosion.

CONCLUSIONS

The overpressure from a vapour cloud explosion cannot be quantified with great accuracy by any method now available. Understanding of the processes involved is developing rapidly, however, and current knowledge can be used to provide valuable guidance for the assessment of explosion hazards in congested plant. The method presented here is an extension of the approach developed by Cates (1), based on analysis of recent experimental data and computation. Support for the use of this methodology comes from analysis of explosion incidents (3).

ACKNOWLEDGEMENTS

The author gratefully acknowledges the contributions made to the analyses presented in this paper by the numerical simulations of T. Hulek and R.P. Lindstedt, the experimental data obtained by British Gas in the partly CEC-funded MERGE project, and stimulating discussions with Prof. D. Bradley, R.F. Barton and C. Jackson.

REFERENCES

1 A.T. Cates, 1991, Fuel gas explosion guidelines. Int. Conf. on Fire and Explosion Hazards, Moreton-in-the-Marsh, Inst. Energy.

2 I.Chem.E., 1994, Overpressure Monograph.

3 R.F Barton, 1995, Fuel gas explosion guidelines - practical applications. Second European Conference on Major Hazards On- and Off-shore, Manchester, 24th - 26th October, 1995, to be presented.

4 A.T. Cates and B. Samuels, 1991, A simple assessment methodology for vented explosions. J. Loss Prev. Process Ind., **4**, 287-294.

5 A.C. van den Berg, 1985, The multi-energy method: a framework for vapour cloud explosion blast prediction. J. Hazardous Materials, **12**, 1-10.

6 A.C. van den Berg, C.J.M. van Wingerden and H.G. The, 1991, Vapor Cloud Explosion Blast Modeling. In: Proc. Intl. Conf. Modeling and Mitigating the Consequences of Accidental Releases of Hazardous Materials, New Orleans, May 1991.

7 W.P.M. Mercx, (ed.), 1993, Modelling and Experimental Research into Gas Explosions, Overall final report of the MERGE project, CEC contract STEP-CT-0111(SSMA).

8 G.A. Shale, 1993, Project MERGE medium and large scale explosion experiments. Report to CEC, British Gas plc., Loughborough.

9 W.P.M. Mercx, D.M. Johnson and J.S. Puttock, 1994, Validation of scaling techniques for experimental vapour cloud explosion investigations. Process Safety Progress, **14**, 120-130.

10 A.J. Harrison and J.A. Eyre, 1987, The effect of obstacle arrays on the combustion of large premixed gas/air clouds. Comb. Sci. Tech., **52**, 121-137.

11 Det norske Veritas, 1982-3 Reports on "Gas explosion research programme", (unpublished).

12 P.H. Taylor and W.J.S. Hirst, 1988, The scaling of vapour cloud explosions: a fractal model for size and fuel type. 22nd. Symp. (Intl.) on Combustion.

13 T. Hulek and R.P. Lindstedt, 1994, Private communication.

Table 1

Fuel	Fuel factor F
methane	0.6
toluene	0.7
pentane	1.0
cyclohexane	1.0
butane	1.0
propane	1.0
methanol	1.0
acetone	1.0
benzene	1.0
ethanol	1.5
propylene (propene)	1.5
butadiene	2
ethylene (ethene)	3

APPENDIX

The Congestion Assessment Method - Guidelines

The method consists of three parts. The first two assist the user in estimating the overpressure in an explosion, while the third part estimates overpressures at a distance. It is stressed that these guidelines should be read in conjunction with the discussion in the main text on vapour cloud explosions. Some judgement from the user is required in using this document. The main aim of the first part is to establish situations where the overpressure generated by an explosion (assuming propane-like fuel) can safely be assumed to be less than the 1 bar default usually taken by the multi-energy method. For hazard areas where a more accurate overpressure estimate is needed, programs are under development which may eventually predict overpressures with reasonable confidence.

A decision tree (see next page) is used for assessing likely "source" overpressures for vapour cloud explosions. Individual geometries generally require expert assessment, and the figures derived from the decision tree may be decreased in some cases on consideration of the detailed layout.

The overpressure, P_{ref}, derived is based on propane-like hydrocarbons (that is hydrocarbons with a similar expansion ratio and laminar flame speed to propane, such as butane). Next the "fuel factor", F, for the fuel in question should be obtained from Table 1. Set

$$P_0 = F \times P_{ref}$$

A volume, V, should then be derived, as an estimate for the volume of compressed gas generated by the explosion. Detailed consideration of the geometry can often reduce the volume which should be taken into account, but by default the total volume of gas within 2m of any obstacle should be calculated, and **should be doubled**. (N.B. This doubling is not a safety precaution; in practice a large part of the explosion will take place in turbulent gas driven outside the confined area.) It is perfectly legitimate for the explosion from a long narrow hazard area to be treated as several simultaneous spherical explosions of appropriate fractions of the total volume, provided the resulting pressures are added up.

Calculate $R_0 = \sqrt[3]{\frac{3V}{2\pi}}$.

At a distance r' from the *edge* of the hazard area, the overpressure should be taken either simply as

$$P = \left(\frac{R_0}{r' + R_0}\right) P_0$$

or calculated from the more comprehensive formulation in Equation 4 or Figure 5. Note that the peak pressure of the front face of a building may be doubled or more by pressure wave reflection. For $r' < R_0$, the dynamic pressure may also be significant, and "edge of the hazard area" should be carefully defined to allow for the expansion of the explosion source beyond the congested region. (See the discussion of both these points in the Section headed "The Method in Practice").

DECISION TREE

Start

Is the hazard area, or any part of the hazard area, more than 60% enclosed by walls, roof, obstacles etc.?

Yes — Seek specialist advice on venting and blow-out panels

No

Are there any obstacles at all in the hazard area? ("No" means that the area is completely open)

No — Assume $P_{ref} = 0.1$

Yes

Are there any small, nearly enclosed areas where ignition may take place?

Yes — There may be a risk of "bang-box" ignition and high pressures. See discussion in main text.

No

Is there any place from where the easiest route for gas to get to an unconfined area involves passing four or more successive obstacles?

No — Assume $P_{ref} = 0.2$

Yes

Note how much gap (for the gas to pass through) there is between the obstacles, and divide by the obstacle diameter to get s_1; also divide the space between successive obstacles by the diameter to get S_2. Let $S = S_1 \times S_2$. P_{ref} depends on S and the number of obstacle rows as follows:

$S > 30$	Obstacle rows:	4-5	6-7	8	> 8
	P_{ref}:	0.3	0.7	1.0	★
$7 < S < 30$	Obstacle rows:	4-5	6	>6	
	P_{ref}:	0.7	1.0	★	
$S < 7$	★				

★ Seek specialist advice.

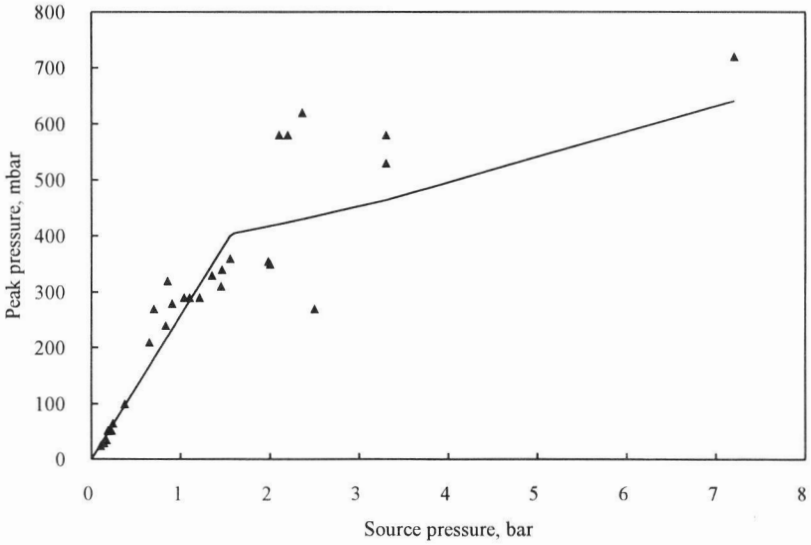

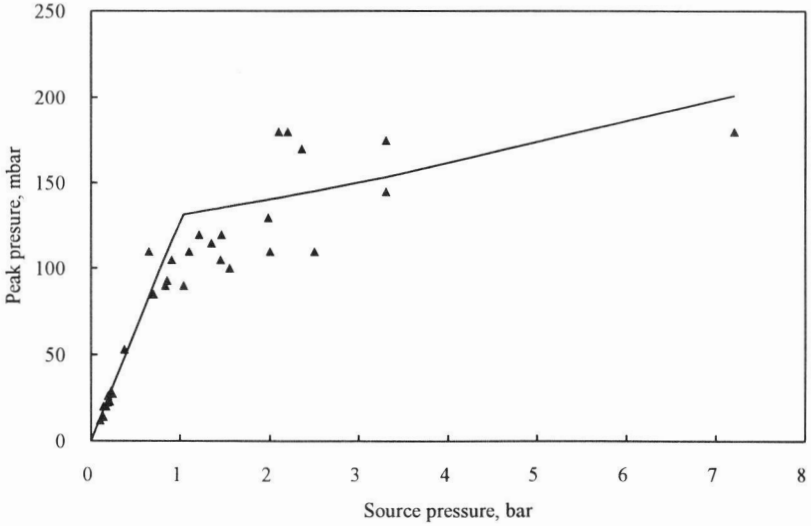

Figure 1 Peak pressure measured at (a) 12m and (b) 24m in the MERGE experiments (24m and 48m at large scale), plotted as a function of peak pressure at the source.

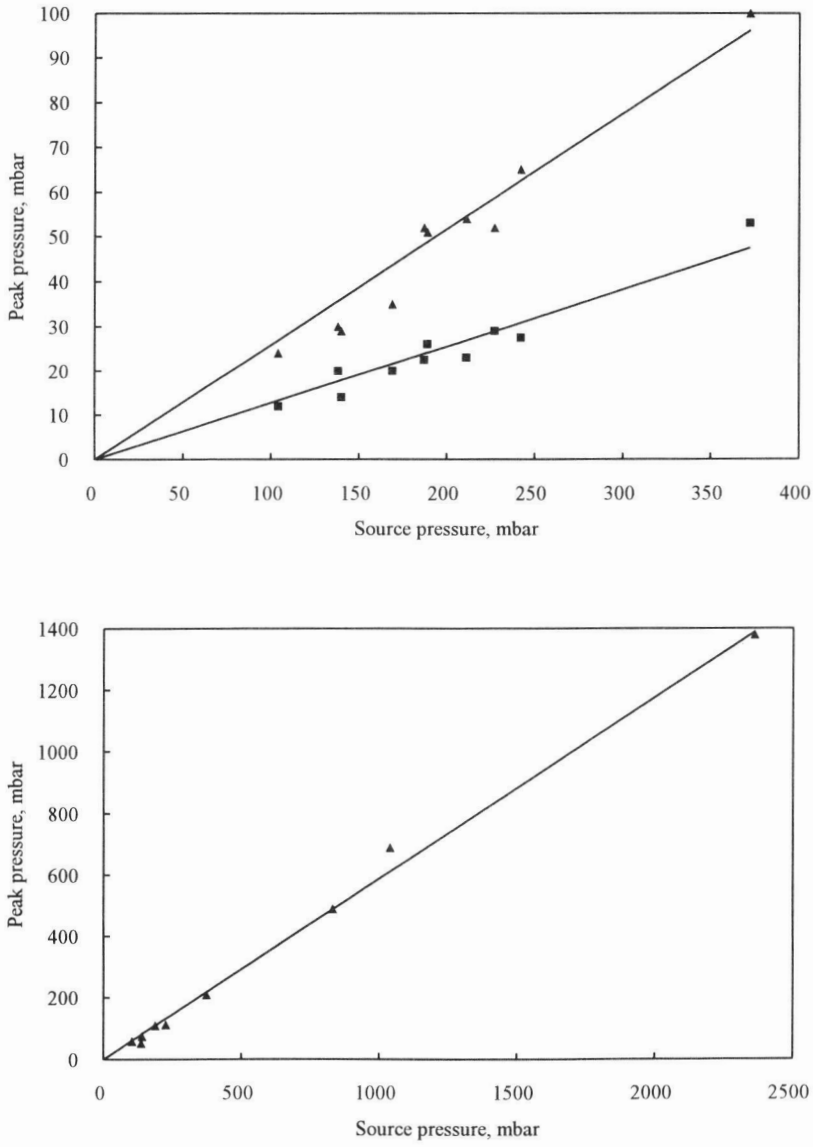

Figure 2 Peak pressure measured in the MERGE medium- and large-scale experiments at (a) 12m and 24m for source pressure < 400mbar, and (b) 4m, plotted as a function of peak pressure at the source.

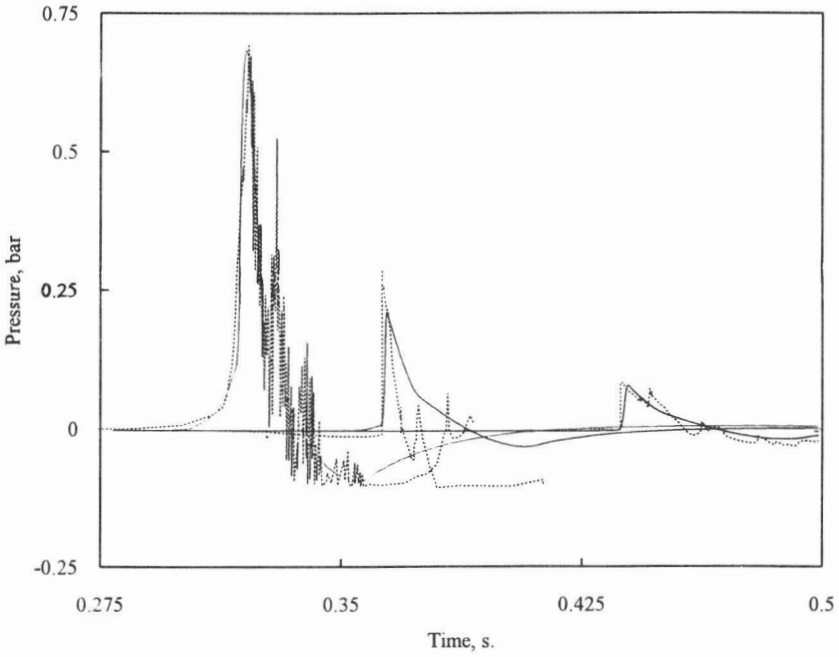

Figure 3 External pressure measurements in MERGE experiment L5, with the profile fitted at 8m for Hulek and Lindstedt's numerical simulations, and the numerical predictions at 24m and 48m.

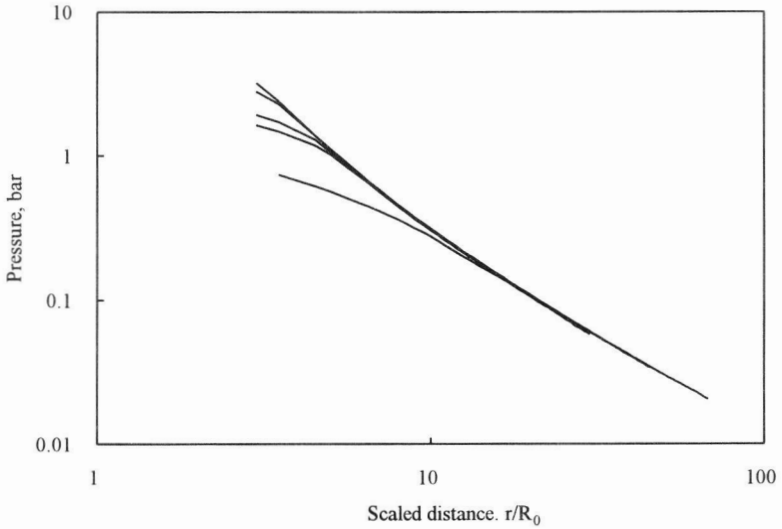

Figure 4 By shifting laterally, the pressure decay curves from the five numerical simulations can be made to coincide, apart from the initial decay.

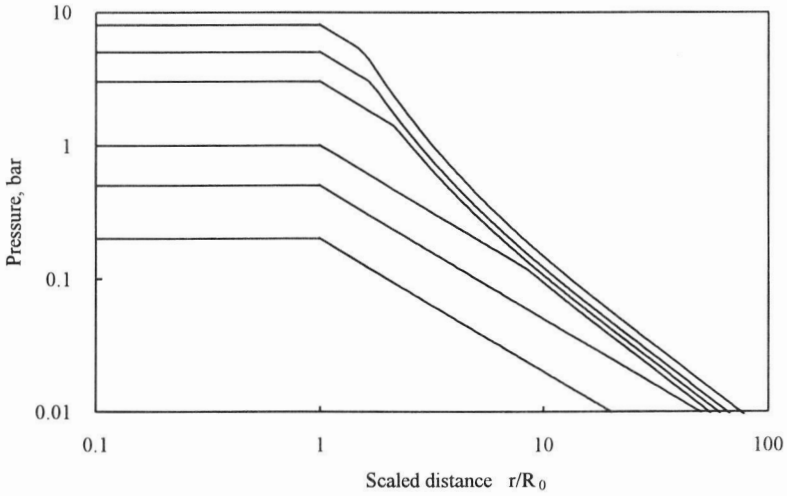

Figure 5 The pressure decay curves given by Equation 4 for source pressure (P) of 0.2, 0.5, 1, 3 5 and 8 bar

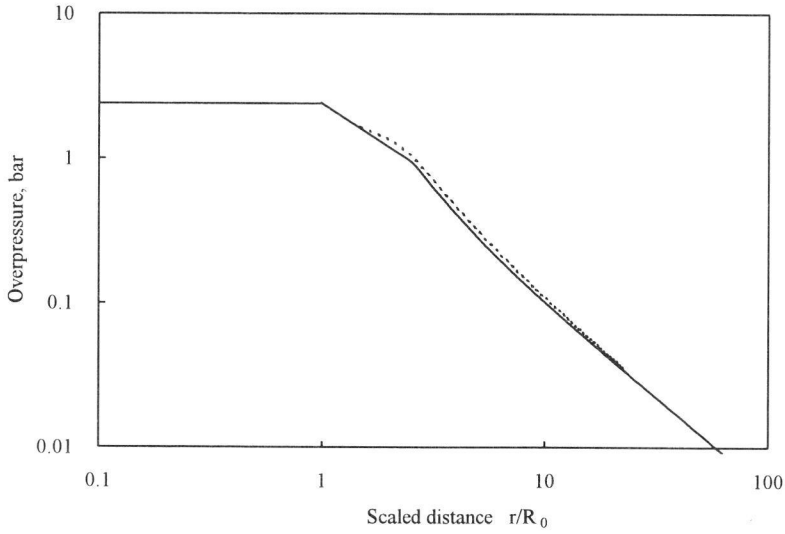

Figure 6 Comparison of the simplified pressure decay curve (Equation 4, Figure 5) with the detailed computation for MERGE experiment L6 (dashed line).

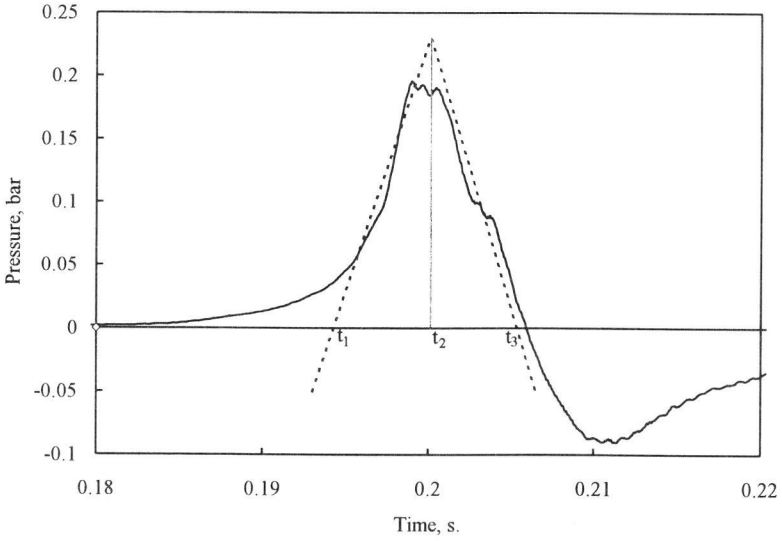

Figure 7 An example of a triangle fitted to the positive part of a pressure trace

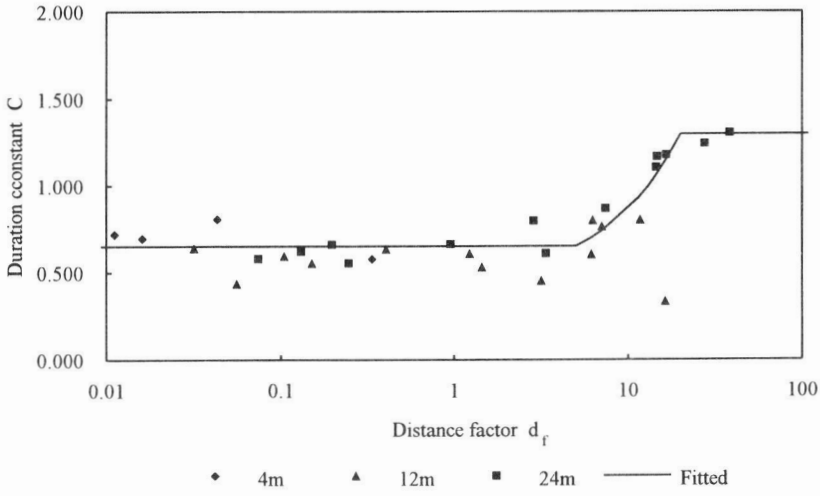

Figure 8 The duration constant expression (Equation 7) fitted to the MERGE data. A logarithmic axis is used, as the data can then be seen much more clearly, but the consequence is that the straight line fit appears as a curve (also in Figure 9).

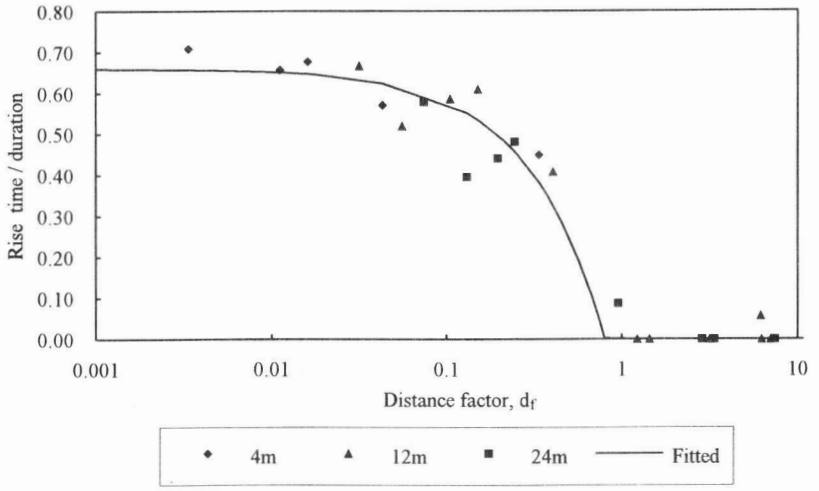

Figure 9 The shape factor (rise time/duration) for the positive part of the pressure pulse: MERGE data and fitted line.